

Decouple and Track: Benchmarking and Improving Video Diffusion Transformers For Motion Transfer

Qingyu Shi¹ Jianzong Wu¹ Jinbin Bai³ Jiangning Zhang⁴ Lu Qi⁵ Xiangtai Li² Yunhai Tong¹
¹ PKU ² NTU ³ NUS ⁴ ZJU ⁵ UC Merced

Project page: <https://shi-qingyu.github.io/DeT.github.io>



Figure 1. We explore the use of Diffusion Transformers (DiT) for the motion transfer task. Compared to previous works, our DeT accurately transfers motion from the source video while flexibly controlling both the foreground and background. Additionally, we highlight the worst-generated regions with red boxes.

Abstract

The motion transfer task involves transferring motion from a source video to newly generated videos, requiring the model to decouple motion from appearance. Previous diffusion-based methods primarily rely on separate spatial and temporal attention mechanisms within 3D U-Net. In contrast, state-of-the-art video Diffusion Transformers (DiT) models use 3D full attention, which does not explicitly separate temporal and spatial information. Thus, the interaction between spatial and temporal dimensions makes decoupling motion and appearance more challenging for DiT models. In this paper, we propose DeT, a method that

adapts DiT models to improve motion transfer ability. Our approach introduces a simple yet effective temporal kernel to smooth DiT features along the temporal dimension, facilitating the decoupling of foreground motion from background appearance. Meanwhile, the temporal kernel effectively captures temporal variations in DiT features, which are closely related to motion. Moreover, we introduce explicit supervision along dense trajectories in the latent feature space to further enhance motion consistency. Additionally, we present MTBench, a general and challenging benchmark for motion transfer. We also introduce a hybrid motion fidelity metric that considers both the global and local motion similarity. Therefore, our work provides a more

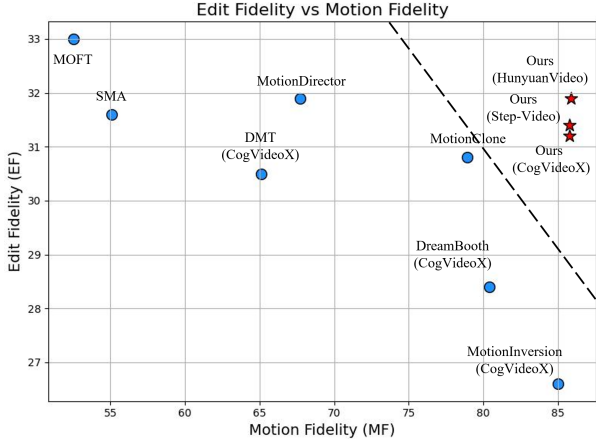


Figure 2. **Method comparison.** Our method exhibits the best balance between motion fidelity and edit fidelity.

comprehensive evaluation than previous works. Extensive experiments on MTBench demonstrate that DeT achieves the best trade-off between motion fidelity and edit fidelity.

1. Introduction

The advancement of foundation models for text-to-video generation has driven significant breakthroughs [7, 8, 17, 18, 26, 50]. Notably, Diffusion Transformers (DiT) video generation models have achieved remarkable results [33, 37, 59, 63]. However, generating complex motion remains a challenging, and relying solely on text prompts often fails to meet user expectations. To address this limitation, the motion transfer [23, 30, 60] seeks to generate videos that adhere to the motion in the source video under text control. This enables users to customize motion while retaining control over the foreground and background.

The main challenge of this task is to decouple the motion from the appearance in the source video. Previous methods [24, 42, 62] mainly relied on separated temporal and spatial self-attention in 3D U-Net models [44], with spatial self-attention being frozen during motion learning for decoupling. However, these approaches are incompatible with the recent state-of-the-art DiT models [29], as their 3D full attention mechanism [59] does not explicitly separate temporal and spatial information. The interaction of spatial and temporal dimensions in 3D attention makes the decoupling of motion and appearance more challenging. Furthermore, in terms of the benchmark, to the best of our knowledge, previous evaluation benchmarks [30, 60] are not general enough. Previous evaluation benchmarks include only basic motion, such as straight-line movements [60]. These benchmarks composed of simple motions fails to comprehensively evaluate the capability of motion transfer methods, limiting their practical applicability.

In this paper, we leverage the superior performance of DiT models for the motion transfer task and introduce a general motion transfer benchmark and a hybrid metric to evaluate motion fidelity. We first implement two existing methods, MotionInversion and DreamBooth [45, 48], which are compatible with DiT models as baselines. Through toy experiments shown in Fig. 3 (a), we observe that these baselines struggle to control the background through text. By visualizing the outputs of 3D full attention in Fig. 3. We find that foreground and background features are difficult to distinguish, indicating that foreground motion and background appearance are not correctly decoupled. We argue that this is due to the temporal inconsistencies of the background feature in the denoising process, as shown in Fig. 4. This makes it challenging to differentiate between foreground and background in specific frames. To encourage the model to decouple background appearance from foreground motion, we smooth the feature in 3D full attention along the temporal dimension. This facilitates a more precise separation between foreground and background. On the other hand, to learn motion accurately, we examine the 3D attention map and find that significant attention scores appear primarily along the diagonal for adjacent frames. This observation motivates us to adopt a temporal 1D kernel to learn temporal information while simultaneously decoupling foreground appearance. The temporal kernel also effectively smooths features across time. By applying a trainable shared temporal kernel, we achieve motion alignment while ensuring the decoupling of both foreground and background appearance. Considering the correspondence of optical flow in both pixel and feature spaces [47], we further enhance foreground motion consistency by introducing explicit supervision on latent features, named dense point tracking loss. The dense point tracking loss aligns features along the foreground’s trajectories, encouraging the model to generate consistent motion dynamics.

Furthermore, we propose a larger and more general benchmark dubbed MTBench. To meet the requirements for foreground-centric content and dynamic motion, MTBench is sourced from two publicly available datasets [40, 57]. We select 100 high-quality videos and leverage recent Multimodal Large Language Model [4], Large Language Model [58], and tracking model [25] for video annotation. We generate five evaluation prompts for each source video and annotate foreground trajectories. The initial points for the trajectories are sampled from the mask using distance-weighted sampling. So the isolated point is more likely to be sampled. This ensures sampling within narrow but important regions such as limbs. An automatic clustering algorithm [12] is then applied to group the trajectories, categorizing the motions into three difficulty levels based on the number of clusters. In addition, we also propose a hybrid motion fidelity metric. Instead of relying solely on the

similarity between local velocity [60] of trajectories, we introduce Fréchet distance [13] to measure the alignment of their global shape. With general MTBench and the hybrid motion fidelity metric, our work offers a more comprehensive evaluation of motion transfer methods.

Building on MTBench, both qualitative and quantitative results highlight the superior performance of our method in achieving an optimal balance between motion and edit fidelity. Further ablation studies confirm the effectiveness of our proposed shared temporal kernel and dense point tracking loss. Notably, as shown in Fig. 1, our approach is good at transferring the motion between cross-category foregrounds, resulting in a more generalized motion transfer method. To summarize, our key contributions include:

- An effective method that decouples and learns motion patterns simultaneously.
- We introduce a dense point tracking loss in the latent space to enhance foreground motion consistency.
- A challenging and comprehensive benchmark for the motion transfer task, dubbed MTBench.
- A hybrid metric for evaluating motion fidelity.
- We achieve the best trade-off between motion and edit fidelity on MTBench as shown in Fig. 2.

2. Related Work

Text-to-video diffusion models. Building on recent text-to-image (T2I) diffusion models [3, 9, 14, 38, 43], early approaches [8, 17] extended pre-trained T2I models to generate dynamic videos. These methods typically incorporate temporal self-attention within the U-Net [44] architecture to ensure motion dynamics. However, due to the per-patch computation, the generated videos often exhibit temporal inconsistencies in motion. Recently, the DiT models [19, 29, 33, 59] introduced 3D Full Attention, and through end-to-end training on large-scale video datasets [5, 11], it is capable of generating temporally consistent and high-quality videos. However, generating motion solely from text prompts remains challenging, particularly when it comes to meeting user demands for complex motions. In this paper, we propose a novel method that enables users to generate specific motions within a source video under text control.

Motion transfer. This task aims to transfer the motion from a source video to a generated video. Unlike video editing tasks [1, 2, 10, 15, 16, 31, 34, 54], motion transfer focuses solely on the motion pattern in the source video, allowing for more flexible control of the foreground and background in the generated video through text. The main challenge in motion transfer is decoupling motion from appearance in the source video, enabling effective learning of the motion while avoiding memorizing appearance. Previous methods [24, 36, 42, 48, 62] relied on a U-Net architecture with a decoupled spatial and temporal self-attention

mechanism. They fine-tune the parameters in the temporal self-attention only to ensure the motion is learned without overfitting. However, the state-of-the-art DiT models [29] use 3D full attention without explicit spatial temporal decoupling, making previous approaches incompatible with DiT models. We propose the shared temporal kernel and dense point tracking loss to decouple and track motion in the source video, enabling DiT models to effectively transfer it to newly generated video.

3. Method

Given a source video \mathcal{S} and a text prompt P , our goal is to generate a new video \mathcal{J} that retains the overall motion of \mathcal{S} while aligning with P . In the following section, we first introduce two baseline approaches and examine their weaknesses, and then we present our method to decouple motion from appearance in \mathcal{S} .

3.1. Motivations

Since previous works only fine-tune temporal attention in 3D U-Net [23, 24, 36, 42, 52], they are not compatible with DiT models. As baselines, we implement the embedding-based method MotionInversion [48] and the fully fine-tuned method DreamBooth [45] on DiT models. As shown in Fig. 3 (a), neither method effectively controls the appearance of the foreground and background using text. Moreover, the entangled motion and appearance information further complicates motion learning.

To investigate this issue and dig out reasons, we extract the output of 3D full attention, referred to as the DiT feature $\mathcal{I} \in \mathbb{R}^{thw \times c}$, where t, h, w are compressed frames, height, and width respectively. We visualize \mathcal{I} using Principle Component Analysis (PCA) in Fig. 3 (a). The results reveal that foreground and background features are difficult to distinguish, suggesting that background appearance and foreground motion are not properly decoupled. Consequently, when generating foreground motion, the background appearance becomes entangled with it.

To address this issue, we analyze the DiT feature \mathcal{I} during the denoising process. As shown in Fig. 4, we observe that temporal inconsistencies in *background features* make distinguishing between foreground and background challenging. To separate foreground and background, an ideal approach is to smooth foreground and background features along the temporal dimension. Additionally, in order to accurately learn the motion pattern. We analyze the 3D attention map. The fig. 5 shows that strong diagonal attention scores appear only in adjacent frames. This suggests that modeling temporal changes in DiT features does not depend on the spatial receptive field and should instead focus on *local temporal* information. The reduction of spatial dimension also encourages the model to decouple the foreground appearance. Based on the above analysis, leveraging

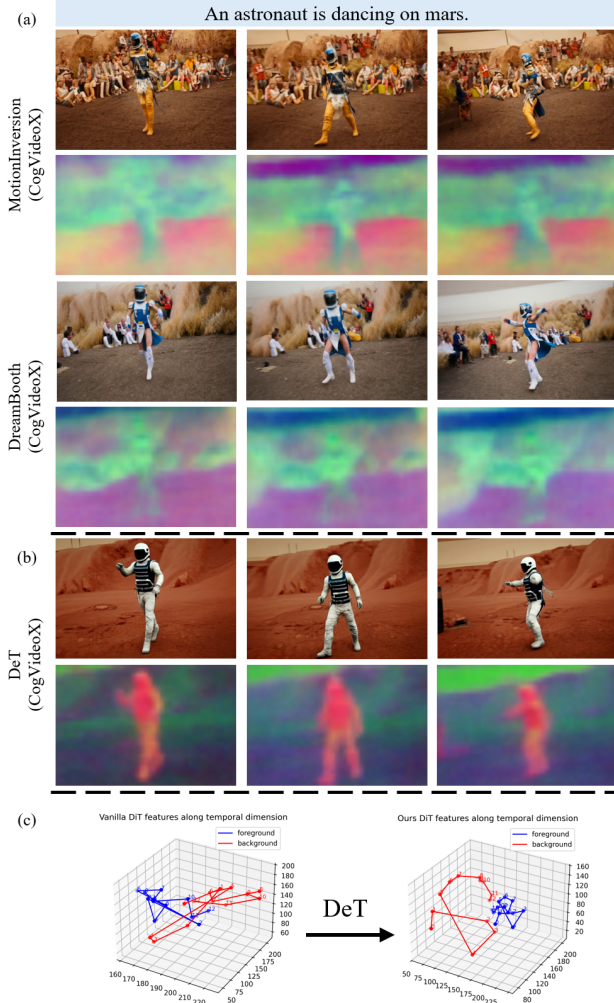


Figure 3. Comparison of DiT features. The source video is shown in Fig. 4. We use CogVideoX-5B as the default model, extracting and averaging DiT features from the 4th block across all denoising steps. (a) and (b) is the baseline and our method’s generated frames and DiT features, respectively. (c) Illustrate the DiT feature along the temporal dimension.

smoothness and temporal learning enables the decoupling of both foreground and background appearance, leading to successful motion transfer.

3.2. DeT

Shared temporal kernel. Building on the motivation, we first apply temporal smoothness to the reshaped DiT features $\mathcal{I}' \in \mathbb{R}^{hw \times t \times c}$. Specifically, we use a temporal kernel $\mathcal{K}^t \in \mathbb{R}^{k \times c \times c}$ to perform convolution along the temporal dimension. From a manifold learning perspective, the temporal kernel functions as an equivalent Laplacian smoothing

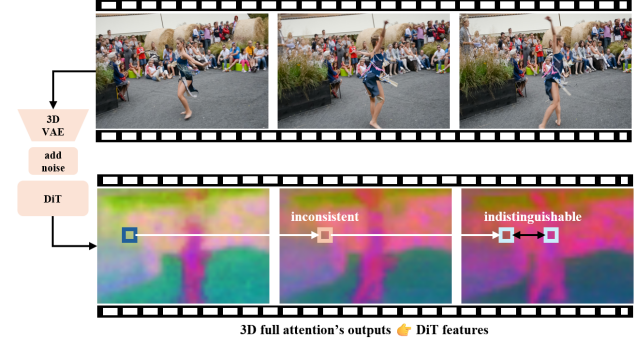


Figure 4. The visualization of DiT features. We attribute the failure to decouple background appearance to the difficulty of distinguishing foreground and background features in certain frames. As a result, background appearance becomes entangled with foreground motion during training.

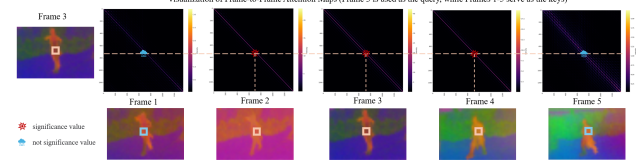


Figure 5. The visualization of frame-to-frame attention map. We mark significant and non-significant values in the figure. Significant values appear only along the diagonal of adjacent frames, suggesting that capturing DiT feature changes over time requires only a local temporal receptive field, not a spatial one.

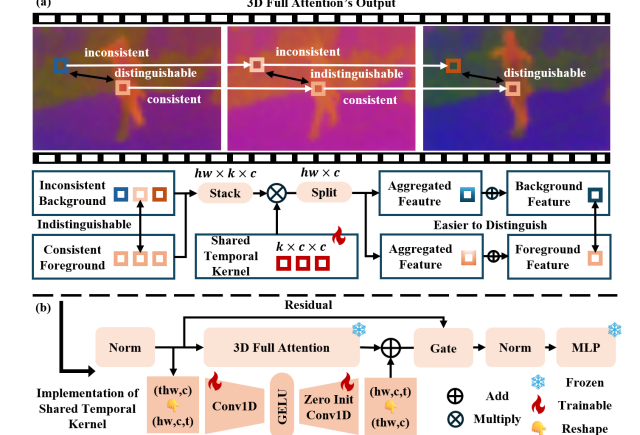


Figure 6. Overview of the shared temporal kernel. Figure (a) illustrates the smoothing mechanism of the shared temporal kernel, which aggregates DiT features along the temporal dimension. Figure (b) presents its implementation using temporal 1D convolution with a GELU activation function.

operator along the temporal axis:

$$\hat{\mathcal{I}}_{xy, i} = \mathcal{I}'_{xy, i} + \sum_{j=-\frac{k-1}{2}}^{\frac{k-1}{2}} \mathcal{I}'_{xy, i+j} \times \mathcal{K}_j^t \quad (1)$$

, where xy and i represent the spatial and temporal coordinates, respectively. After applying smoothness, the model can utilize the refined temporal trajectories to achieve more

	DMT [60]	MotionDirector [62]	MotionClone [30]	SMA [36]	MTBench
Num Videos	21	76	40	30	100
Num Prompts	56	228	Unknown	Unknown	500
Benchmark Source	DAVIS [40] & Web Source	LOVEU-TGVE [55]	DAVIS [40] & Web Source	DAVIS [40] & WebVid10M [5]	DAVIS [40] & YouTube-VOS [57]
Domain	Animal & Vehicle	Human & Animal & Vehicle	Human & Animal & Vehicle	Human & Animal & Vehicle	Human & Animal & Vehicle
Difficulty	Easy	Easy & Medium	Easy & Medium	Easy & Medium	Easy & Medium & Hard
Num Clusters	2.57	4.72	4.13	3.91	6.31

Table 1. **Benchmark Comparison.** We present a table summarizing the scale and difficulty of previous benchmarks.

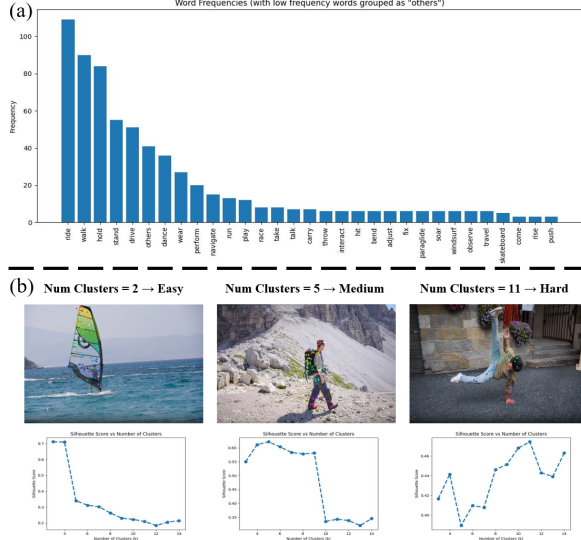


Figure 7. **Overview of MTBench.** (a) illustrates the motion frequency distribution in evaluation prompts. (b) illustrates difficulty levels based on the number of trajectory clusters: 1-3 as easy, 4-6 as medium, and 7+ as hard.

reliable differentiation.

Furthermore, we find that the temporal kernel also serves as an ideal model for motion learning. As discussed above, motion learning primarily depends on local temporal information rather than a spatial receptive field. The shared temporal kernel along the spatial dimension effectively meets both requirements. Thus, we incorporate it into all DiT blocks. Specifically, as shown in Fig. 6, to enhance efficiency and reduce memory consumption, we adopt a down-and-up architecture $\mathcal{K}_{down}^t \in \mathbb{R}^{k \times c \times m}$, $\mathcal{K}_{up}^t \in \mathbb{R}^{k \times m \times c}$ with a GELU activation σ function in the middle:

$$\tilde{\mathcal{I}} = \mathcal{K}_{up}^t * \sigma(\mathcal{K}_{down}^t * \mathcal{I}) + \text{Attention}(\mathcal{I}, \mathcal{E}_{text}) \quad (2)$$

where \mathcal{E}_{text} represents the embedding of the text prompt and $*$ is the convolution operation. As a toy experiment on DiT, Fig. 4 (b) shows that the generated video follows the motion pattern of the source video while maintaining strong text controllability. Furthermore, Fig. 4 (c) demonstrates that our shared temporal kernel effectively enhances the model’s ability to distinguish between foreground and background.

Dense point tracking loss. Inspired by our finding that foreground DiT features remain consistent over time, we introduce more explicit supervision on foreground DiT features along the temporal dimension to enhance the fore-

ground motion consistency.

Specifically, we utilize CoTracker [25] to track the foreground in the source video, generating a set of trajectories $\mathcal{T} \in \mathbb{R}^{N \times T \times 2}$, where N denotes the number of trajectories. Additionally, CoTracker provides the visibility of each point in the form of $\mathcal{V} \in \{0, 1\}^{N \times T \times 1}$, where 1 indicates visibility, and 0 denotes invisibility. During the training process on source video \mathcal{S} , we calculate dense point tracking loss on the predicted latent feature $\hat{\mathcal{E}}(\mathcal{S}) \in \mathbb{R}^{t \times h \times w \times c}$:

$$\hat{\mathcal{E}}(\mathcal{S}) = \sqrt{\bar{\alpha}_t} \left(\sqrt{\bar{\alpha}_t} \mathcal{E}(\mathcal{S}) + \sqrt{1 - \bar{\alpha}_t} \epsilon \right) - \sqrt{1 - \bar{\alpha}_t} v \quad (3)$$

where $v = \epsilon_\theta \left(\sqrt{\bar{\alpha}_t} \mathcal{E}(\mathcal{S}) + \sqrt{1 - \bar{\alpha}_t} \epsilon \right)$. We align the features along the trajectories \mathcal{T} using the L2 distance. Additionally, to account for occlusions where parts of the trajectory may not be visible, we compute the dense point tracking loss only on visible points by applying \mathcal{V} as a mask:

$$\mathcal{L}_{TL} = \left\| \min(\mathcal{V}(t+1), \mathcal{V}(t)) \times \mathcal{L} \right\|_2^2 \quad (4)$$

where $\mathcal{L} = \hat{\mathcal{E}}(\mathcal{S})[\mathcal{T}(t+1)] - \hat{\mathcal{E}}(\mathcal{S})[\mathcal{T}(t)]$. The final loss is a combination of denoising loss (DL) and dense point tracking loss (TL), weighted by λ_{DL} and λ_{TL} :

$$\mathcal{L} = \lambda_{DL} \mathcal{L}_{DL} + \lambda_{TL} \mathcal{L}_{TL} \quad (5)$$

3.3. MTBench

3.3.1. Data Collection and Annotation

As shown in Tab. 1, previous benchmarks fall short in either scale (i.e., number of videos and prompts) or difficulty. To provide a more comprehensive evaluation of the motion transfer method, we construct a more general benchmark based on the DAVIS [40] and YouTube-VOS [57] datasets, which includes 100 high-quality videos with 500 evaluation prompts. We use the Qwen2.5-VL-7B [4] to annotate captions for the videos. Based on each caption, we generate five evaluation text prompts using the Qwen2.5-14B [58], swapping the foreground and background while keeping the verb unchanged. Additionally, we use the SAM [28] and CoTracker [25] to annotate masks and trajectories for the subjects in the videos. We then perform automatic K-means clustering of all trajectories based on the silhouette coefficient [12]. The motion in each video is categorized into easy, medium, and hard levels based on the number of clusters. We visualize the motion distribution in evaluation prompts and present examples of the difficulty division



Figure 8. **Qualitative results of DeT.** The left column of videos is generated by CogVideoX-5B, while the right column is generated by HunyuanVideo. DeT can transfer motion from easy to hard difficulty levels. The generated video adheres to the motion pattern of the source video while allowing flexible foreground and background control through text.

in Fig. 7 (a) and (b). We compared our benchmark with previous works in Tab. 1, showcasing the diverse range of motions it includes.

3.3.2. Metric

Hybrid motion fidelity (motion fidelity, for short). We introduce Fréchet distance d_F [13] to compare the shape differences between trajectories $\mathcal{T}_i, \mathcal{T}_j \in \mathbb{R}^{N \times T \times 2}$. It considers both the spatial arrangement and the order of points. This ensures that the transferred motion globally adheres to the source motion. We also use cosine similarity [60] to compare the local velocity direction $\Delta\mathcal{T}(t) = \mathcal{T}(t+1) - \mathcal{T}(t)$. Specifically, we compute motion fidelity

score \mathcal{M} through the formulation:

$$\mathcal{M}(\mathcal{T}_i, \mathcal{T}_j) = \frac{1}{N} \sum_{n=1}^N \left[\alpha e^{-d_F(\mathcal{T}_i^n, \mathcal{T}_j^n)} + (1 - \alpha) \bar{c}_n \right],$$

where $\bar{c}_n = \frac{1}{T-1} \sum_{t=1}^{T-1} \cos(\Delta\mathcal{T}_i^n(t), \Delta\mathcal{T}_j^n(t))$, and $\alpha \in [0, 1]$ is a weighting parameter that balances the shape and velocity similarity. We set $\alpha = 0.5$ in our experiments.

Edit fidelity. Following previous works [20, 22, 45]. We use CLIP [41] to measure the similarity between each frame and the target text prompt, reporting the average score.

Temporal consistency. The motion learning process may cause temporal flickering. We compute the cosine similarity



Figure 9. **Qualitative comparison.** We compare DeT with other state-of-the-art motion transfer methods. We specify the base models used in parentheses. DeT demonstrates a clear advantage in both motion and edit fidelity.

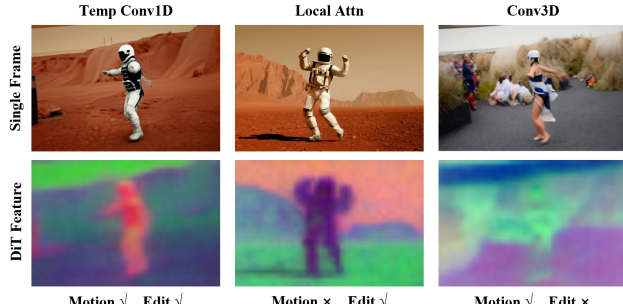


Figure 10. **Ablation study on shared temporal kernel.** Temporal kernel achieve both motion fidelity and edit fidelity.

between the DINO [35] features of consecutive frames to measure the temporal consistency of the generated videos.

4. Experiment

4.1. Experimental Setup

Implementation details. We apply DeT on three pre-trained DiT models—CogVideoX-5B [59], Hunyuan-Video [29], and StepVideo-T2V [33] to demonstrate its generalization capabilities. We just provide implementation details for CogVideoX as the base model in the main paper. For HunyuanVideo and Step-Video-T2V, please refer to the Supplementary Material (SM). We train DeT for 500 steps



Figure 11. **Ablation study on dense point tracking loss.** We visualize the cosine similarity across video frames.

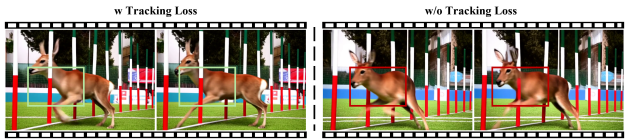


Figure 12. **Ablation study on dense point tracking loss.** Improvements are highlighted using green and red boxes.

on a single source video using the AdamW optimizer [27] with a learning rate of 1e-5 and a weight decay of 1e-2. The loss weight parameters λ_{DL} and λ_{TL} is set to 1.0 and 0.1. The mid-dimension is set to 128 for the shared temporal kernel, and the kernel size is configured to 3. During training, we integrate the shared temporal kernel into all DiT blocks. During inference, we remove the shared temporal

Method	All			Hard			Medium			Easy		
	EF	TC	MF									
MotionDirector	<u>31.9</u>	91.7	67.7	<u>32.3</u>	<u>88.3</u>	67.9	<u>32.5</u>	<u>93.4</u>	66.8	30.8	93.4	68.3
SMA	31.6	82.9	55.1	32.9	78.1	44.1	32.1	84.7	52.1	29.9	85.8	69.2
MotionClone	30.8	80.9	78.9	30.5	74.4	72.5	31.9	83.4	79.2	30.0	84.8	<u>85.0</u>
MOFT	33.0	91.1	52.5	33.8	89.7	48.0	33.2	92.1	53.2	31.9	91.4	56.3
DMT (CogVideoX)	30.5	87.6	65.1	31.6	84.1	64.1	31.8	89.0	64.6	28.2	89.6	66.7
DreamBooth (CogVideoX)	28.4	85.6	80.4	27.5	83.2	76.9	27.9	84.7	80.1	29.9	88.9	84.2
MotionInversion (CogVideoX)	26.6	85.4	85.0	27.2	80.8	80.7	27.2	84.9	90.8	25.5	89.4	84.6
Ours (CogVideoX)	31.2	89.6	85.8	31.8	84.7	80.3	31.1	91.5	92.2	30.7	92.7	84.8
Ours (HunyuanVideo)	<u>31.9</u>	91.9	85.9	31.1	89.7	80.1	32.3	93.1	92.2	31.1	<u>92.9</u>	85.4
Ours (Step-Video-T2V)	31.4	91.6	85.8	30.9	87.6	<u>80.5</u>	31.7	93.5	91.9	<u>31.6</u>	92.7	<u>85.0</u>

Table 2. **Quantitative results on MTBench.** We denote EF: Edit Fidelity, TC: Temporal Consistency, MF: Motion Fidelity.

kernel from the last 27 blocks (65%). This operation improves edit fidelity, as explained in the SM. The injected shared temporal kernel efficiently transfers motion from the source video to the generated video under text control. We perform 50-step denoising using the DDIM scheduler and set the classifier-free guidance scale to 6.0. The generated videos are $49 \times 480 \times 720$. The training process finishes in around 1 hour in a single NVIDIA A100 GPU.

Baselines. We compare our method with state-of-the-art motion transfer methods, including MotionDirector [62], SMA [36], MOFT [56], and MotionClone [30]. Since previous motion transfer methods are based on 3D U-Net and cannot be directly applied to DiT, we implement DMT [60], MotionInversion [48], and DreamBooth [45] on DiT model to ensure a fair comparison.

4.2. Qualitative Results

As shown in Fig. 8, our method accurately transfers the motion from the source video without overfitting to the appearance. This enables flexible text control over both the foreground and background. Additionally, our method supports motion transfer across different categories, such as from a human to a panda or from a train to a boat. In Fig. 1 and Fig. 9, we compare our approach with previous motion transfer methods. U-Net-based methods [36, 62] struggle to maintain motion fidelity and exhibit weak text editing fidelity. We also adapt MotionInversion [48], DMT [60], and DreamBooth [45] to DiT [59]. However, we observe that Motion Inversion suffers from overfitting, failing to edit a rider into an astronaut or modify the background. DreamBooth and DMT fails to capture accurate motion patterns, causing originally curved motion trajectories to become linear. In contrast, our method accurately transfers motion patterns while allowing flexible text-based control over both the foreground and background appearance.

Method	Edit Fidelity	Temporal Consistency	Motion Fidelity
LoRA	28.4	85.6	<u>80.4</u>
Conv3D	27.1	87.4	84.9
Local Attn	<u>31.3</u>	<u>88.2</u>	73.1
Temp Conv1D	31.6	90.4	85.6

Table 3. **Ablation on different motion learning methods.**

Percent	EF	TC	MF	λ_{TL}	EF	TC	MF
75%	<u>31.3</u>	89.4	83.1	1e-1	31.6	90.4	85.6
65%	31.6	90.4	85.6	1e-2	31.6	<u>90.2</u>	<u>83.4</u>
55%	30.4	<u>90.3</u>	<u>85.2</u>	w/o TL	<u>31.2</u>	89.6	82.3
(a) Ablation study on the percentage of dropped layers.						(b) Ablation study on the weight of dense point tracking loss λ_{TL} .	
k	EF	TC	MF	m	EF	TC	MF
3	31.6	90.4	85.6	64	<u>31.7</u>	<u>90.1</u>	84.2
5	<u>31.1</u>	89.3	<u>83.1</u>	128	<u>31.6</u>	90.4	85.6
7	30.7	<u>89.6</u>	81.7	256	30.9	89.9	82.6
(c) Ablation study on the kernel size k of shared temporal kernel.						(d) Ablation study on the mid dim m of shared temporal kernel.	

Table 4. **Ablation studies on the hyperparameters in DeT.**

4.3. Quantitative Results

The quantitative results on MTBench are shown in Tab. 2. Our method with HunyuanVideo achieves the highest Motion Fidelity. While MOFT is slightly higher in edit fidelity, our method achieves the best balance between edit and motion fidelity. Additionally, we adapt MotionInversion, DreamBooth, and DMT to the DiT model, all of which underperform compared to our method across all metrics. Furthermore, in previous works, motion fidelity decreases as difficulty increases, while edit fidelity improves. This indicates that our benchmark difficulty division is reasonable. Notably, our method achieves the highest score on the medium difficulty level, which we attribute to its significant performance improvement in this level.

4.4. Ablation Study

Shared temporal kernel. We conduct the ablation study on the key design choices. Instead of using a shard temporal kernel, we consider alternative approaches through LoRA [21], Conv3D, and local attention [32]. As shown in Tab. 3, our method achieves the best performance in edit and motion fidelity metrics. Fig. 10 shows that shared temporal kernel achieve decoupling while learning the motion. We attribute our success to effective temporal smoothness and an attention map-based motion learning method. Additionally, we ablate the percentage of dropped layers, kernel size, and middle dimension in Tab. 4a, Tab. 4c, and Tab. 4d, respectively. Quantitative results show that dropping 65% of layers, using a kernel size of 3, and setting the middle dimension to 128 achieve the best performance.

Dense point tracking loss. In Tab. 4b, we ablate the weight of the dense point tracking loss and find that $\lambda_{TL} = 1e-1$ achieves the best results. Figure 11 illustrates the cosine similarity between DiT features during training. The dense point tracking loss facilitates precise foreground tracking. Additionally, as shown in Fig. 12, we conduct a qualitative comparison for removing the dense point tracking loss. The green and red boxes highlight the effect of dense point tracking loss, which enhances the motion consistency.

5. Conclusion

We propose DeT, a tuning-based method that leverages DiT models for the motion transfer task. Our novel shared temporal kernel effectively decouples and learns the motion simultaneously. We further introduce dense point tracking loss on latent features to further enhance the foreground motion’s consistency. Additionally, we propose MTBench, a more challenging and general benchmark with a hybrid motion fidelity metric combining Fréchet distance with velocity similarity. Experimental results demonstrate DeT’s effectiveness in accurately transferring motion while maintaining strong text controllability.

Acknowledgement. This work is supported by the National Key Research and Development Program of China (No. 2023YFC3807600).

References

- [1] Jinbin Bai, Zhen Dong, Aosong Feng, Xiao Zhang, Tian Ye, Kaicheng Zhou, and Mike Zheng Shou. Integrating view conditions for image synthesis. *arXiv preprint arXiv:2310.16002*, 2023. 3
- [2] Jinbin Bai, Wei Chow, Ling Yang, Xiangtai Li, Juncheng Li, Hanwang Zhang, and Shuicheng Yan. Humanedit: A high-quality human-rewarded dataset for instruction-based image editing. *arXiv preprint arXiv:2412.04280*, 2024. 3
- [3] Jinbin Bai, Tian Ye, Wei Chow, Enxin Song, Qing-Guo Chen, Xiangtai Li, Zhen Dong, Lei Zhu, and Shuicheng Yan. Meis sonic: Revitalizing masked generative transformers for efficient high-resolution text-to-image synthesis. *arXiv preprint arXiv:2410.08261*, 2024. 3
- [4] Shuai Bai, Keqin Chen, Xuejing Liu, Jialin Wang, Wenbin Ge, Sibo Song, Kai Dang, Shijie Wang, Peng Wang, Jun Tang, Humen Zhong, Yuanzhi Zhu, Mingkun Yang, Zhao-hai Li, Jianqiang Wan, Wei Wang, Pengfei Ding, Zheren Fu, Yiheng Xu, Jiabo Ye, Xi Zhang, Tianbao Xie, Zesen Cheng, Hang Zhang, Zhibo Yang, Haiyang Xu, and Junyang Lin. Qwen2.5-vl technical report. *arXiv preprint arXiv:2502.13923*, 2025. 2, 5
- [5] Max Bain, Arsha Nagrani, Gülcin Varol, and Andrew Zisserman. Frozen in time: A joint video and image encoder for end-to-end retrieval. In *ICCV*, 2021. 3, 5
- [6] Andreas Blattmann, Tim Dockhorn, Sumith Kulal, Daniel Mendelevitch, Maciej Kilian, Dominik Lorenz, Yam Levi, Zion English, Vikram Voleti, Adam Letts, Varun Jampani, and Robin Rombach. Stable video diffusion: Scaling latent video diffusion models to large datasets. *arXiv preprint arXiv:2311.15127*, 2023. 9
- [7] Andreas Blattmann, Robin Rombach, Huan Ling, Tim Dockhorn, Seung Wook Kim, Sanja Fidler, and Karsten Kreis. Align your latents: High-resolution video synthesis with latent diffusion models. In *CVPR*, 2023. 2, 9
- [8] Haoxin Chen, Yong Zhang, Xiaodong Cun, Menghan Xia, Xintao Wang, Chao Weng, and Ying Shan. Videocrafter2: Overcoming data limitations for high-quality video diffusion models. In *CVPR*, 2024. 2, 3
- [9] Junsong Chen, Jincheng Yu, Chongjian Ge, Lewei Yao, Enze Xie, Yue Wu, Zhongdao Wang, James Kwok, Ping Luo, Huchua Lu, and Zhenguo Li. Pixart- α : Fast training of diffusion transformer for photorealistic text-to-image synthesis. In *ICLR*, 2023. 3
- [10] Pengtao Chen, Mingzhu Shen, Peng Ye, Jianjian Cao, Chongjun Tu, Christos-Savvas Bouganis, Yiren Zhao, and Tao Chen. δ -dit: A training-free acceleration method tailored for diffusion transformers. *arXiv preprint arXiv:2406.01125*, 2024. 3
- [11] Tsai-Shien Chen, Aliaksandr Siarohin, Willi Menapace, Ekaterina Deyneka, Hsiang-wei Chao, Byung Eun Jeon, Yuwei Fang, Hsin-Ying Lee, Jian Ren, Ming-Hsuan Yang, et al. Panda-70m: Captioning 70m videos with multiple cross-modality teachers. In *CVPR*, 2024. 3
- [12] Duy-Tai Dinh, Tsutomu Fujinami, and Van-Nam Huynh. Estimating the optimal number of clusters in categorical data clustering by silhouette coefficient. In *Knowledge and Systems Sciences: 20th International Symposium, KSS 2019, Da Nang, Vietnam, November 29–December 1, 2019, Proceedings 20*, pages 1–17. Springer, 2019. 2, 5
- [13] Thomas Eiter and Heikki Mannila. Computing discrete fréchet distance. *Technical Report CD-TR 94/64, Christian Doppler Laboratory for Expert*, 1994. 3, 6
- [14] Patrick Esser, Sumith Kulal, Andreas Blattmann, Rahim Entezari, Jonas Müller, Harry Saini, Yam Levi, Dominik Lorenz, Axel Sauer, Frederic Boesel, Dustin Podell, Tim Dockhorn, Zion English, Kyle Lacey, Alex Goodwin, Yannik Marek, and Robin Rombach. Scaling rectified flow trans-

- formers for high-resolution image synthesis. In *ICML*, 2024.
- [15] Aosong Feng, Weikang Qiu, Jinbin Bai, Kaicheng Zhou, Zhen Dong, Xiao Zhang, Rex Ying, and Leandros Tassiulas. An item is worth a prompt: Versatile image editing with disentangled control. *arXiv preprint arXiv:2403.04880*, 2024.
- [16] Michal Geyer, Omer Bar-Tal, Shai Bagon, and Tali Dekel. Tokenflow: Consistent diffusion features for consistent video editing. In *ICLR*, 2024.
- [17] Yuwei Guo, Ceyuan Yang, Anyi Rao, Zhengyang Liang, Yaohui Wang, Yu Qiao, Maneesh Agrawala, Dahua Lin, and Bo Dai. Animatediff: Animate your personalized text-to-image diffusion models without specific tuning. In *ICLR*, 2024.
- [18] Agrim Gupta, Lijun Yu, Kihyuk Sohn, Xiuye Gu, Meera Hahn, Li Fei-Fei, Irfan Essa, Lu Jiang, and José Lezama. Photorealistic video generation with diffusion models. *arXiv preprint arxiv:2312.06662*, 2023.
- [19] Yoav HaCohen, Nisan Chiprut, Benny Brazowski, Daniel Shalem, Dudu Moshe, Eitan Richardson, Eran Levin, Guy Shiran, Nir Zabari, Ori Gordon, et al. Ltx-video: Realtime video latent diffusion. *arXiv preprint arXiv:2501.00103*, 2024.
- [20] Jack Hessel, Ari Holtzman, Maxwell Forbes, Ronan Le Bras, and Yejin Choi. Clipscore: A reference-free evaluation metric for image captioning. In *EMNLP*, 2021.
- [21] Edward J. Hu, Yelong Shen, Phillip Wallis, Zeyuan Allen-Zhu, Yuanzhi Li, Shean Wang, Lu Wang, and Weizhu Chen. Lora: Low-rank adaptation of large language models. In *ICLR*, 2022.
- [22] Ziqi Huang, Yinan He, Jiahuo Yu, Fan Zhang, Chenyang Si, Yuming Jiang, Yuanhan Zhang, Tianxing Wu, Qingyang Jin, Nattapol Chanpaisit, Yaohui Wang, Xinyuan Chen, Limin Wang, Dahua Lin, and Ziwei Qiao, Yu andLiu. VBench: Comprehensive benchmark suite for video generative models. In *CVPR*, 2024.
- [23] Hyeonho Jeong, Jinho Chang, Geon Yeong Park, and Jong Chul Ye. Dreammotion: Space-time self-similar score distillation for zero-shot video editing. In *ECCV*, 2024.
- [24] Hyeonho Jeong, Geon Yeong Park, and Jong Chul Ye. Vmc: Video motion customization using temporal attention adaptation for text-to-video diffusion models. In *CVPR*, 2024.
- [25] Nikita Karaev, Ignacio Rocco, Benjamin Graham, Natalia Neverova, Andrea Vedaldi, and Christian Rupprecht. Co-tracker: It is better to track together. In *ECCV*, 2024.
- [26] Levon Khachatryan, Andranik Movsisyan, Vahram Tadevosyan, Roberto Henschel, Zhangyang Wang, Shant Navasardyan, and Humphrey Shi. Text2video-zero: Text-to-image diffusion models are zero-shot video generators. In *ICCV*, 2023.
- [27] Diederik Kingma and Jimmy Ba. Adam: A method for stochastic optimization. In *ICLR*, 2015.
- [28] Alexander Kirillov, Eric Mintun, Nikhila Ravi, Hanzi Mao, Chloe Rolland, Laura Gustafson, Tete Xiao, Spencer Whitehead, Alexander C Berg, Wan-Yen Lo, et al. Segment anything. In *ICCV*, 2023.
- [29] Weijie Kong, Qi Tian, Zijian Zhang, Rox Min, Zuozhuo Dai, Jin Zhou, Jiangfeng Xiong, Xin Li, Bo Wu, Jianwei Zhang, et al. Hunyuanyvideo: A systematic framework for large video generative models. *arXiv preprint arXiv:2412.03603*, 2024.
- [30] Pengyang Ling, Jiazi Bu, Pan Zhang, Xiaoyi Dong, Yuhang Zang, Tong Wu, Huaiyan Chen, Jiaqi Wang, and Yi Jin. Motionclone: Training-free motion cloning for controllable video generation. *arXiv preprint arXiv:2406.05338*, 2024.
- [31] Shaoteng Liu, Yuechen Zhang, Wenbo Li, Zhe Lin, and Jiaya Jia. Video-p2p: Video editing with cross-attention control. In *CVPR*, 2024.
- [32] Ze Liu, Yutong Lin, Yue Cao, Han Hu, Yixuan Wei, Zheng Zhang, Stephen Lin, and Baining Guo. Swin transformer: Hierarchical vision transformer using shifted windows. In *ICCV*, 2021.
- [33] Guoqing Ma, Haoyang Huang, Kun Yan, Liangyu Chen, Nan Duan, Shengming Yin, Changyi Wan, Ranchen Ming, Xiaoniu Song, Xing Chen, et al. Step-video-t2v technical report: The practice, challenges, and future of video foundation model. *arXiv preprint arXiv:2502.10248*, 2025.
- [34] Chenlin Meng, Yutong He, Yang Song, Jiaming Song, Ji-jun Wu, Jun-Yan Zhu, and Stefano Ermon. Sdedit: Guided image synthesis and editing with stochastic differential equations. In *ICLR*, 2022.
- [35] Maxime Oquab, Timothée Darcet, Theo Moutakanni, Huy V. Vo, Marc Szafraniec, Vasil Khalidov, Pierre Fernandez, Daniel Haziza, Francisco Massa, Alaaeldin El-Nouby, Russell Howes, Po-Yao Huang, Hu Xu, Vasu Sharma, Shang-Wen Li, Wojciech Galuba, Mike Rabbat, Mido Assran, Nicolas Ballas, Gabriel Synnaeve, Ishan Misra, Herve Jegou, Julien Mairal, Patrick Labatut, Armand Joulin, and Piotr Bojanowski. Dinov2: Learning robust visual features without supervision, 2023.
- [36] Geon Yeong Park, Hyeonho Jeong, Sang Wan Lee, and Jong Chul Ye. Spectral motion alignment for video motion transfer using diffusion models. In *AAAI*, 2025.
- [37] William Peebles and Saining Xie. Scalable diffusion models with transformers. In *CVPR*, 2023.
- [38] Dustin Podell, Zion English, Kyle Lacey, Andreas Blattmann, Tim Dockhorn, Jonas Müller, Joe Penna, and Robin Rombach. Sdxl: Improving latent diffusion models for high-resolution image synthesis. In *ICLR*, 2024.
- [39] Adam Polyak, Amit Zohar, Andrew Brown, Andros Tjandra, Animesh Sinha, Ann Lee, Apoorv Vyas, Bowen Shi, Chih-Yao Ma, Ching-Yao Chuang, et al. Movie gen: A cast of media foundation models. *arXiv preprint arXiv:2410.13720*, 2024.
- [40] Jordi Pont-Tuset, Federico Perazzi, Sergi Caelles, Pablo Arbeláez, Alex Sorkine-Hornung, and Luc Van Gool. The 2017 davis challenge on video object segmentation. *arXiv preprint arXiv:1704.00675*, 2018.
- [41] Alec Radford, Jong Wook Kim, Chris Hallacy, Aditya Ramesh, Gabriel Goh, Sandhini Agarwal, Girish Sastry,

- Amanda Askell an Pamela Mishkin, Jack Clark, Gretchen Krueger, and Ilya Sutskever. Learning transferable visual models from natural language supervision. In *ICML*, 2021. 6
- [42] Yixuan Ren, Yang Zhou, Jimei Yang, Jing Shi, Difan Liu, Feng Liu, Mingi Kwon, and Abhinav Shrivastava. Customize-a-video: One-shot motion customization of text-to-video diffusion models. In *ECCV*, 2024. 2, 3
- [43] Robin Rombach, Andreas Blattmann, Dominik Lorenz, Patrick Esser, and Björn Ommer. High-resolution image synthesis with latent diffusion models. In *CVPR*, 2022. 3
- [44] Olaf Ronneberger, Philipp Fischer, and Thomas Brox. U-net: Convolutional networks for biomedical image segmentation. In *MICCAI*, 2015. 2, 3
- [45] Nataniel Ruiz, Yuanzhen Li, Varun Jampani, Yael Pritch, Michael Rubinstein, and Kfir Aberman. Dreambooth: Fine tuning text-to-image diffusion models for subject-driven generation. In *CVPR*, 2023. 2, 3, 6, 8
- [46] Qingyu Shi, Lu Qi, Jianzong Wu, Jinbin Bai, Jingbo Wang, Yunhai Tong, Xiangtai Li, and Ming-Husan Yang. Relationbooth: Towards relation-aware customized object generation. *arXiv preprint arXiv:2410.23280*, 2024. 9
- [47] Zachary Teed and Jia Deng. Raft: Recurrent all-pairs field transforms for optical flow. In *ECCV*, 2020. 2
- [48] Luozhou Wang, Ziyang Mai, Guibao Shen, Yixun Liang, Xin Tao, Pengfei Wan, Di Zhang, Yijun Li, and Yingcong Chen. Motion inversion for video customization. *arXiv preprint arXiv:2403.20193*, 2024. 2, 3, 8, 1
- [49] Xiang Wang, Hangjie Yuan, Shiwei Zhang, Dayou Chen, Jiumiu Wang, Yingya Zhang, Yujun Shen, Deli Zhao, and Jingren Zhou. Videocomposer: Compositional video synthesis with motion controllability. In *NeurIPS*, 2023. 9
- [50] Yaohui Wang, Xinyuan Chen, Xin Ma, Shangchen Zhou, Ziqi Huang, Yi Wang, Ceyuan Yang, Yinan He, Jiashuo Yu, Peiqing Yang, et al. Lavie: High-quality video generation with cascaded latent diffusion models. *IJCV*, 2024. 2
- [51] Zhouxia Wang, Ziyang Yuan, Xintao Wang, Tianshui Chen, Menghan Xia, Ping Luo, and Ying Shan. Motionctrl: A unified and flexible motion controller for video generation. In *SIGGRAPH*, 2024. 9
- [52] Yujie Wei, Shiwei Zhang, Zhiwu Qing, Hangjie Yuan, Zhiheng Liu, Yu Liu, Yingya Zhang, Jingren Zhou, and Hongming Shan. Dreamvideo: Composing your dream videos with customized subject and motion. In *CVPR*, 2024. 3, 9
- [53] Jianzong Wu, Xiangtai Li, Yanhong Zeng, Jiangning Zhang, Qianyu Zhou, Yining Li, Yunhai Tong, and Kai Chen. Motionbooth: Motion-aware customized text-to-video generation. *NeurIPS*, 2024. 9
- [54] Jay Zhangjie Wu, Yixiao Ge, Xintao Wang, Weixian Lei, Yuchao Gu, Yufei Shi, Wynne Hsu, Ying Shan, Xiaohu Qie, and Mik Zheng Shou. Tune-a-video: One-shot tuning of image diffusion models for text-to-video generation. In *ICCV*, 2023. 3
- [55] Jay Zhangjie Wu, Xiuyu Li, Difei Gao, Zhen Dong, Jinbin Bai, Aishani Singh, Xiaoyu Xiang, Youzeng Li, Zuwei Huang, Yuanxi Sun, Rui He, Feng Hu, Junhua Hu, Hai Huang, Hanyu Zhu, Xu Cheng, Jie Tang, Mike Zheng Shou, Kurt Keutzer, and Forrest Iandola. Cvpr 2023 text guided video editing competition, 2023. 5
- [56] Zeqi Xiao, Yifan Zhou, Shuai Yang, and Xingang Pan. Video diffusion models are training-free motion interpreter and controller. In *NeurIPS*, 2024. 8
- [57] Ning Xu, Linjie Yang, Yuchen Fan, Dingcheng Yue, Yuchen Liang, Jianchao Yang, and Thomas Huang. Youtube-vos: A large-scale video object segmentation benchmark. *arXiv preprint arXiv:1809.03327*, 2018. 2, 5
- [58] An Yang, Baosong Yang, Beichen Zhang, Binyuan Hui, Bo Zheng, Bowen Yu, Chengyuan Li, Dayiheng Liu, Fei Huang, Haoran Wei, Huan Lin, Jian Yang, Jianhong Tu, Jianwei Zhang, Jianxin Yang, Jiaxi Yang, Jingren Zhou, Junyang Lin, Kai Dang, Keming Lu, Keqin Bao, Kexin Yang, Le Yu, Mei Li, Mingfeng Xue, Pei Zhang, Qin Zhu, Rui Men, Runji Lin, Tianhao Li, Tingyu Xia, Xingzhang Ren, Xuancheng Ren, Yang Fan, Yang Su, Yichang Zhang, Yu Wan, Yuqiong Liu, Zeyu Cui, Zhenru Zhang, and Zihan Qiu. Qwen2.5 technical report. *arXiv preprint arXiv:2412.15115*, 2024. 2, 5
- [59] Zhuoyi Yang, Jiayan Teng, Wendi Zheng, Ming Ding, Shiyu Huang, Jiazheng Xu, Yuanming Yang, Wenyi Hong, Xiaohan Zhang, Guanyu Feng, et al. Cogvideox: Text-to-video diffusion models with an expert transformer. In *ICLR*, 2025. 2, 3, 7, 8, 1
- [60] Danah Yatim, Rafail Fridman, Omer Bar-Tal, Yoni Kasten, and Tali Dekel. Space-time diffusion features for zero-shot text-driven motion transfer. In *CVPR*, 2024. 2, 3, 5, 6, 8, 1
- [61] Shengming Yin, Chenfei Wu, Jian Liang, Jie Shi, Houqiang Li, Gong Ming, and Nan Duan. Dragnuwa: Fine-grained control in video generation by integrating text, image, and trajectory. *arXiv preprint arXiv:2308.08089*, 2023. 9
- [62] Rui Zhao, Yuchao Gu, Jay Zhangjie Wu, David Junhao Zhang, Jiawei Liu, Weijia Wu, Jussi Keppo, and Mike Zheng Shou. Motiondirector: Motion customization of text-to-video diffusion models. In *ECCV*, 2024. 2, 3, 5, 8
- [63] Zangwei Zheng, Xiangyu Peng, Tianji Yang, Chenhui Shen, Shenggui Li, Hongxin Liu, Yukun Zhou, Tianyi Li, and Yang You. Open-sora: Democratizing efficient video production for all. *arXiv preprint arXiv:2412.20404*, 2024. 2
- [64] Qiang Zhou, Shaofeng Zhang, Nianzu Yang, Ye Qian, and Hao Li. Motion control for enhanced complex action video generation. *arXiv preprint arXiv:2411.08328*, 2024. 9

Decouple and Track: Benchmarking and Improving Video Diffusion Transformers For Motion Transfer

Supplementary Material

Overview.

- **Sec. 6.** More qualitative results.
- **Sec. 7.** More qualitative comparison results.
- **Sec. 8.** Implementation details of the experiments.
- **Sec. 9.** Additional analysis and ablation studies.
- **Sec. 10.** Details of the MTBench.
- **Sec. 11.** Additional related works.
- **Sec. 12.** Limitations and future work.

6. More Qualitative Results

We show more qualitative results in Fig. 13, Fig. 14, and Fig. 15. Each source video is combined with two newly generated videos.

7. More Qualitative Comparison Results

We present additional qualitative comparisons in Fig. 16, Fig. 17, and Fig. 18. Our method accurately transfers complex motions while enabling flexible foreground and background control. These results demonstrate the generality of our motion transfer approach.

8. Implementation Details

HunyuanVideo implementation details. We train DeT on HunyuanVideo for 500 steps using the AdamW optimizer with a learning rate of 1e-5 and a weight decay of 1e-2. The learning rate is linearly warmed up over the first 100 steps. The loss weight parameters λ_{DL} and λ_{TL} are set to 1.0 and 0.1, respectively. For the motion module, the mid-dimension is set to 128, and the kernel size is configured to 5. During training, we integrate our shared temporal kernel into all DiT blocks. During inference, we remove it from the last 40 blocks (66%) - all of the single-stream DiT blocks. We perform 30 steps denoising using the Flow Matching scheduler. The generated videos have a resolution of $49 \times 512 \times 768$. The training process takes approximately 1.5 hours on a single NVIDIA A100 80GB GPU.

Step-Video-T2V implementation details. We train DeT on Step-Video-T2V for 500 steps using the AdamW optimizer with a learning rate of 2e-5 and a weight decay of 1e-2. The learning rate is linearly warmed up over the first 100 steps. The loss weight parameters λ_1 and λ_2 are set to 1.0 and 0.1, respectively. For the shared temporal kernel, the mid-dimension is set to 256, and the kernel size is configured to 5. During training, we integrate the shared temporal kernel into all DiT blocks. During inference, we remove it from the last 32 blocks (66%). We perform 50-step

denoising using the Flow Matching (FM) scheduler with a classifier-free guidance scale of 9.0. The generated videos have a resolution of $49 \times 512 \times 768$. The entire training process takes approximately two hours on a single NVIDIA A100 80GB GPU.

Baselines implementation details. We implement MotionInversion [48] on CogVideoX-5B [59] by injecting temporal embeddings $E_t \in \mathbb{R}^{t \times c}$ and spatial embeddings $E_s \in \mathbb{R}^{h \times w \times c}$ into the 3D full attention mechanism. Specifically, we inject E_t into the query and key, while E_s is applied to the value. We train MotionInversion for 500 steps using the AdamW optimizer with a learning rate of 1e-3 and a weight decay of 1e-2, injecting embeddings into all DiT blocks. For DreamBooth, we use the LoRA variant, setting the LoRA rank to 128 and injecting LoRA weights into the query, key, value, and output linear layers. We train with a learning rate of 1e-4 and a weight decay of 1e-2. For DMT, we apply DDIM inversion to each video, which takes approximately one hour. During inference, we extract features from the 28th DiT block and compute SMM [60] via spatial pooling and first-order differencing. The optimization learning rate is set to 1e-2, and we optimize the latents for 20 steps. For other U-Net-based methods, we use their official implementations and settings.

9. Additional Analysis and Ablation Study

9.1. Analysis for drop layers

During inference, we drop the shared temporal kernel in the last 65% of DiT blocks. Experimental results show that this dropping strategy enhances text controllability. We attribute this to the fact that the DiT model relies more on the earlier layers when generating videos, as shown in Fig. 19. This suggests that the shared temporal kernel inserted in the later layers may introduce redundant learnable parameters that capture information unrelated to motion.

Furthermore, the visualization of the attention map in Fig. 20 reveals that in the earlier layers, the DiT model exhibits a mechanism similar to temporal self-attention, whereas the later layers resemble spatiotemporal attention. Spatiotemporal attention is less effective at decoupling motion from appearance, which further supports the decision to drop the temporal kernel in the later layers. Additionally, we observe that applying this layer-dropping strategy consistently improves performance across all three DiT models.

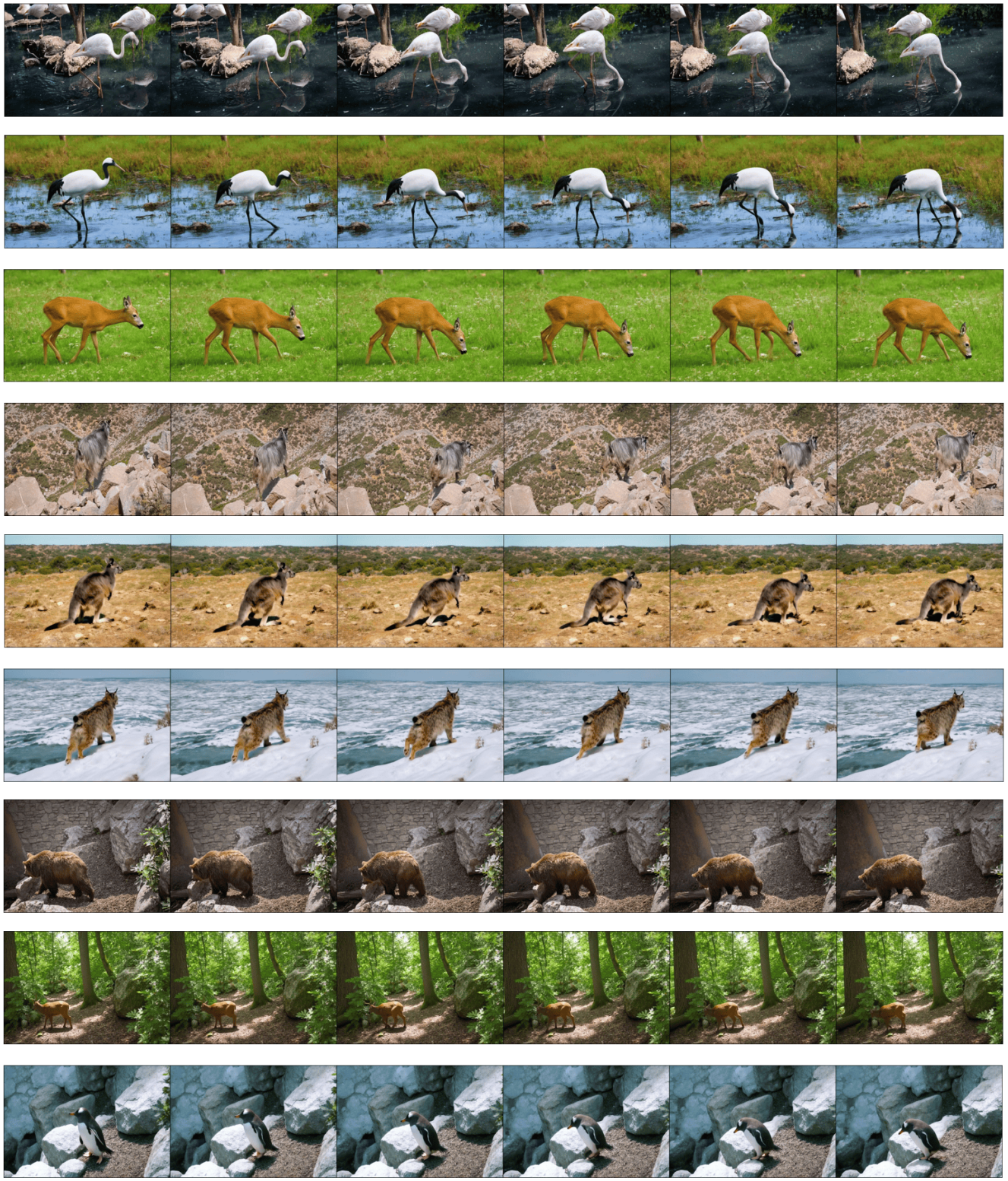


Figure 13. **More Qualitative Results.** There are three set of results. Each source video is combined with two newly generated videos on the bottom. Generated by DeT with Step-Video-T2V

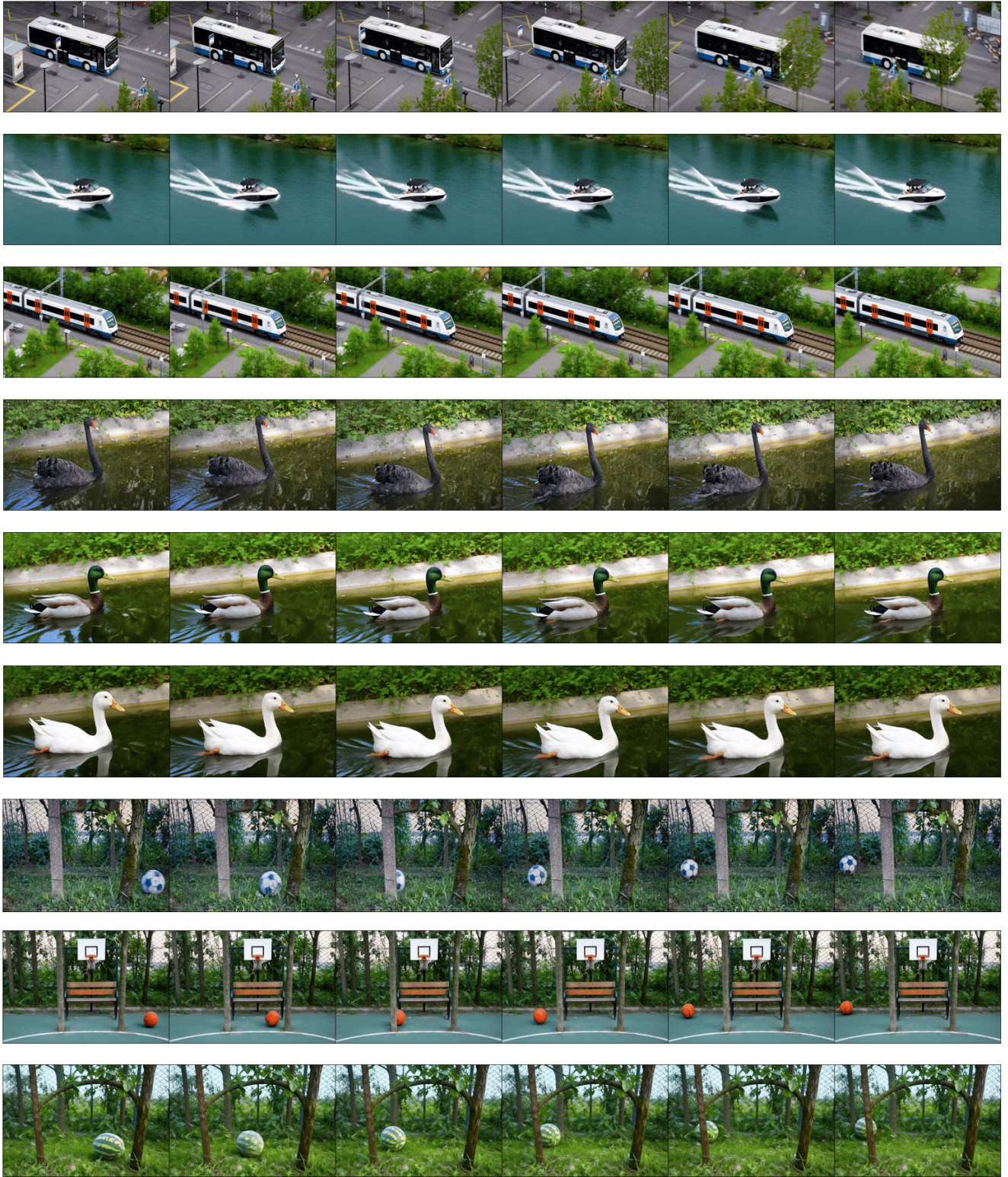


Figure 14. More Qualitative Results. There are three set of results. Each source video is combined with two newly generated videos on the bottom. Generated by DeT with HunyuanVideo

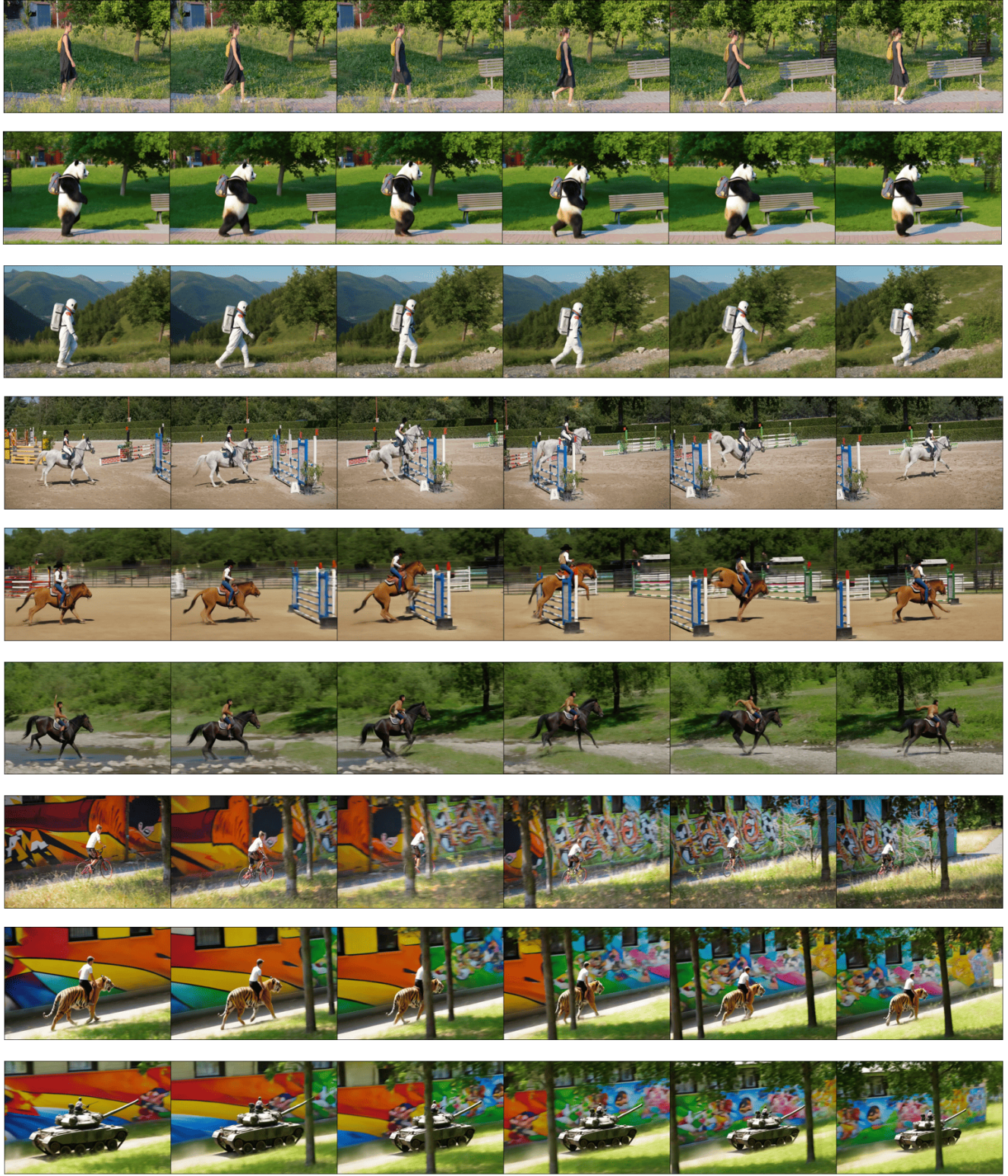


Figure 15. More Qualitative Results. There are three set of results. Each source video is combined with two newly generated videos on the bottom. Generated by DeT with Step-Video-T2V

A woman wearing pink dress is dancing on the ground



A monkey wearing pink dress is dancing on the ground



Ours



DMT



MOFT



MotionClone



MotionDirector



SMA



Figure 16. **More Qualitative Comparision Results.** Our result is generated by DeT with CogVideoX-5B

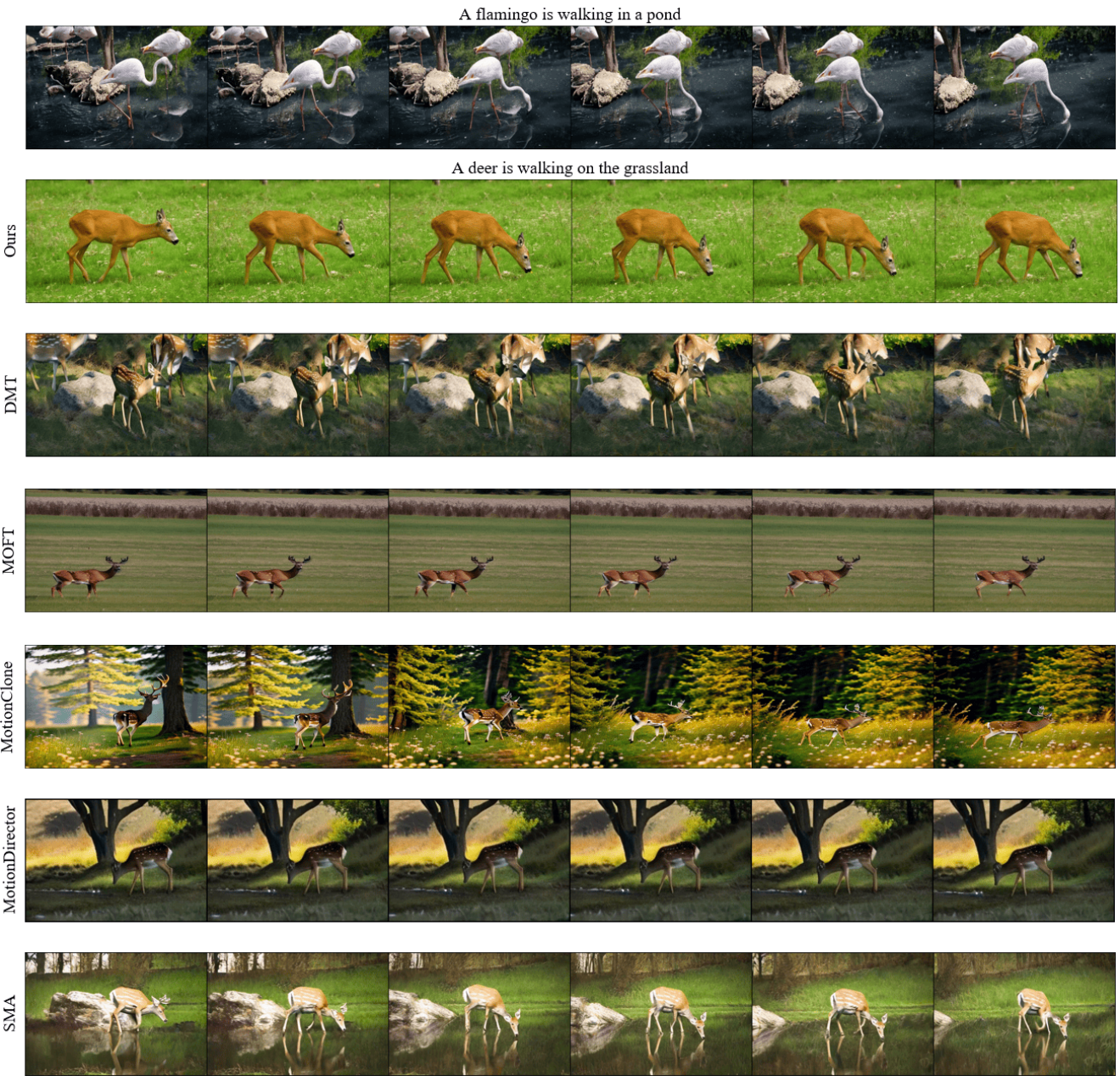


Figure 17. **More Qualitative Comparision Results.** Our result is generated by DeT with Step-Video-T2V

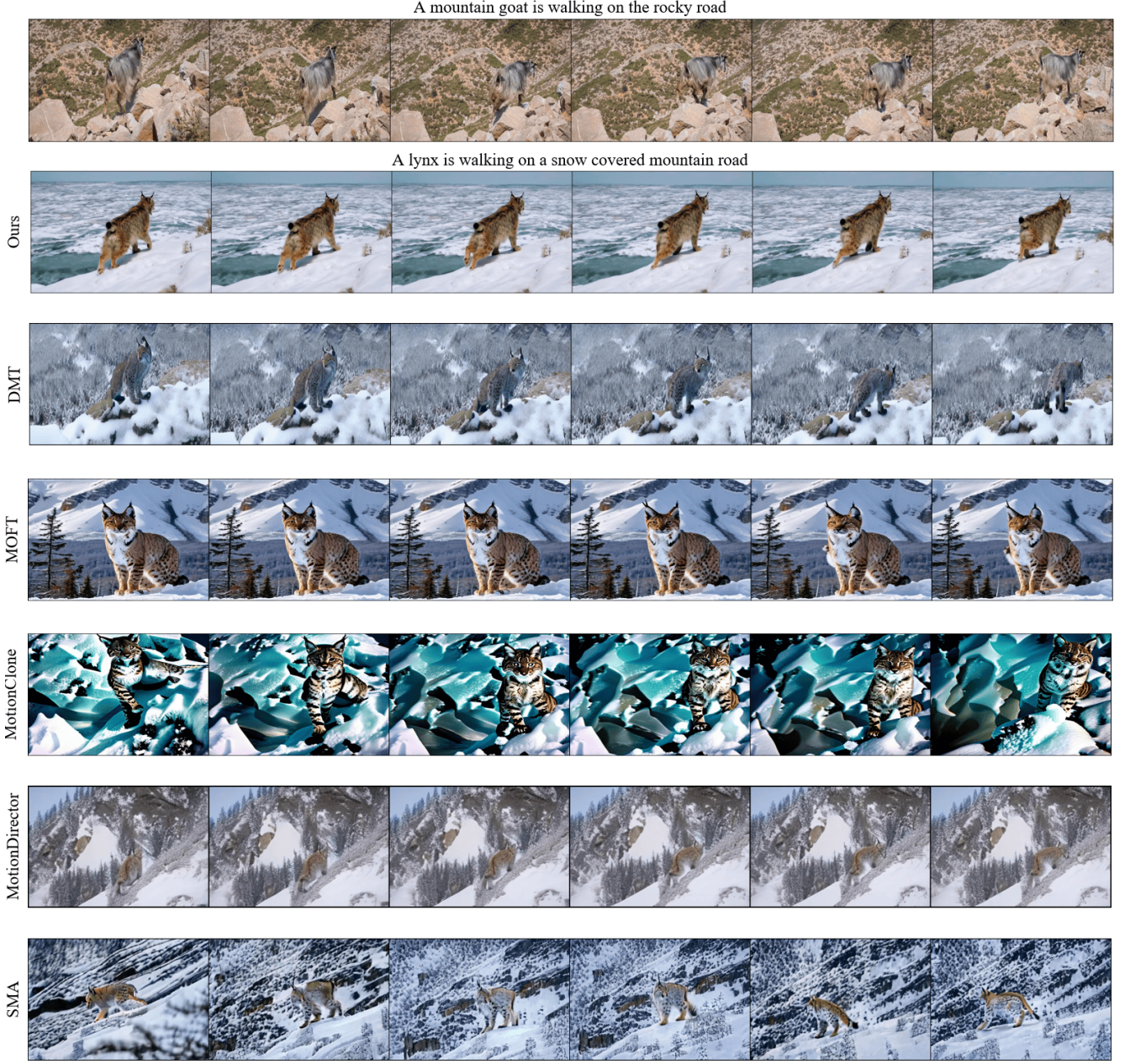


Figure 18. **More Qualitative Comparision Results.** Our result is generated by DeT with Step-Video-T2V

9.2. DeT with HunyuanVideo

Table 5 presents comprehensive ablation studies conducted on various hyperparameters within the DeT framework with HunyuanVideo.

Drop layers. Fig. 5 (a) investigates the impact of varying the percentage of dropped layers. The best performance is achieved at 65%, as indicated by the highest scores. This result highlights the importance of a balanced dropout rate in optimizing the model’s motion transfer capabilities.

Dense point tracking loss. Fig. 5b, we ablate the dense

point tracking loss weight for DeT with HunyuanVideo. We find that $\lambda_{TL} = 1e-1$ achieves the best results.

Temporal kernel size. Fig. 5 (c) ablates the kernel size, with results demonstrating that a kernel size of 5 offers optimal performance. This suggests that the receptive field provided by $k = 5$ strikes the best balance between capturing local temporal dependencies and maintaining computational efficiency.

Mid dimension Fig. 5 (d) explores the mid dimension parameter, showing that a dimension of 128 is most effective.

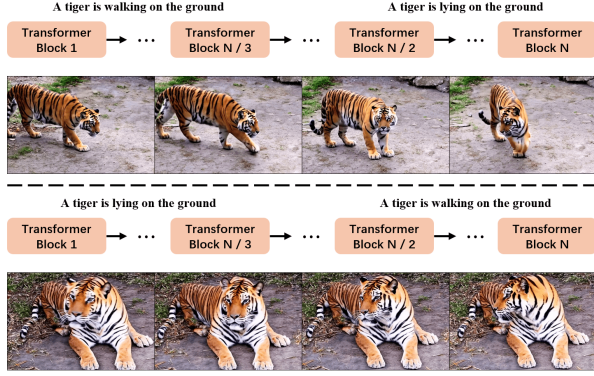


Figure 19. **Analysis of dropping layer strategy.** The generation results of DiT models rely more on features from earlier layers. The tiger’s motion is determined by the text prompt in these early layers.

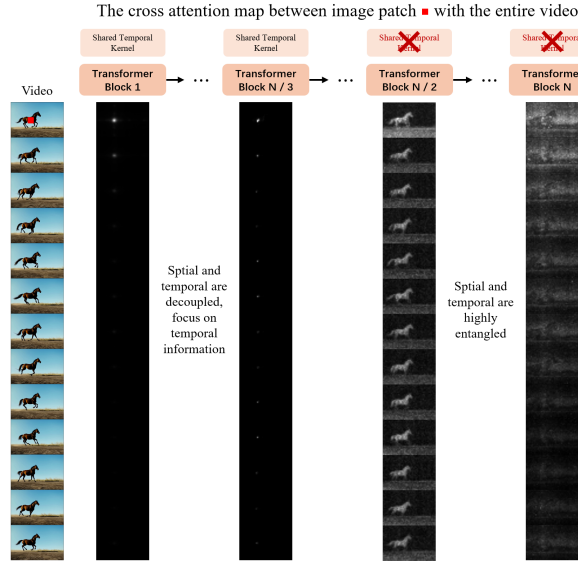


Figure 20. **Anaylsis of dropping layer strategy.** The attention map also supports our dropping layer strategy. As the later layers’ attention maps show entangled spatial and temporal information, decoupling becomes ineffective. To improve decoupling, we remove the shared temporal kernel in these layers.

9.3. DeT with Step-Video-T2V

Table 5 presents comprehensive ablation studies conducted on various hyperparameters within the DeT with Step-Video-T2V.

Drop layers. Table 6a presents the ablation study on the percentage of dropped layers. The best performance is achieved at a 65% drop rate.

Dense point tracking loss. In Table 6b, the impact of the weight λ_{TL} for the dense point tracking loss is evaluated. The results show that setting λ_{TL} to 1e-1 yields the highest performance across all metrics.

Percent	EF	TC	MF	λ_{TL}	EF	TC	MF
75%	31.2	89.1	83.4	1e-1	31.9	91.9	85.9
65%	31.9	91.9	85.9	1e-2	31.7	90.1	84.4
55%	30.7	89.0	85.5	w/o TL	31.6	89.4	83.1

(a) Ablation study on the percentage of dropped layers.

λ_{TL}	EF	TC	MF
1e-1	31.9	91.9	85.9
1e-2	31.7	90.1	84.4
w/o TL	31.6	89.4	83.1

(b) Ablation study on the weight of dense point tracking loss λ_{TL} .

m	EF	TC	MF
64	30.2	90.1	83.2
128	31.9	91.9	85.9
256	30.9	89.9	84.6

(c) Ablation study on the kernel size k of shared temporal kernel.

(d) Ablation study on the mid dim m of shared temporal kernel.

Table 5. Ablation studies on the hyperparameters in DeT with HunyuanVideo.

Percent	EF	TC	MF	λ_{TL}	EF	TC	MF
75%	31.1	88.3	82.3	1e-1	31.4	91.6	85.8
65%	31.4	91.6	85.8	1e-2	30.5	90.5	84.9
55%	30.2	89.0	84.2	w/o TL	31.4	88.5	82.9

(a) Ablation study on the percentage of dropped layers.

k	EF	TC	MF	λ_{TL}	EF	TC	MF
3	31.1	90.1	85.3	1e-1	31.4	91.6	85.8
5	31.4	91.6	85.8	1e-2	30.5	90.5	84.9
7	30.4	88.6	85.4	w/o TL	31.4	88.5	82.9

(c) Ablation study on the kernel size k of shared temporal kernel.

(d) Ablation study on the mid dim m of shared temporal kernel.

Table 6. Ablation studies on the hyperparameters in DeT with Step-Video-T2V.

Temporal kernel size. Table 6c investigates the effect of different kernel sizes for the shared temporal convolution. The experiment reveals that a kernel size of 5 produces the best results, indicating an optimal balance.

Mid dimension Table 6d explores the influence of the mid dimension m of the shared temporal kernel. The performance consistently improves with an increase in m , reaching optimal values when m is set to 256.

10. MTBench Details

MTBench consists of 48 diverse motion categories specifically curated for evaluating motion transfer tasks. We visualize the motion distribution and the number of clusters in MTBench in Fig. 21 and Fig. 22, respectively. Each category is annotated with its occurrence frequency. By incorporating both high-frequency and rare motions, MTBench provides a rigorous assessment of a motion transfer method’s generalization and robustness across a wide range of motion complexities.

Additionally, we visualize the trajectory clusters in Fig. 23. The center of each cluster corresponds to a fundamental movement element of the foreground, such as a bear’s limb. This suggests that aligning the cluster centers of trajectories between the generated and source videos

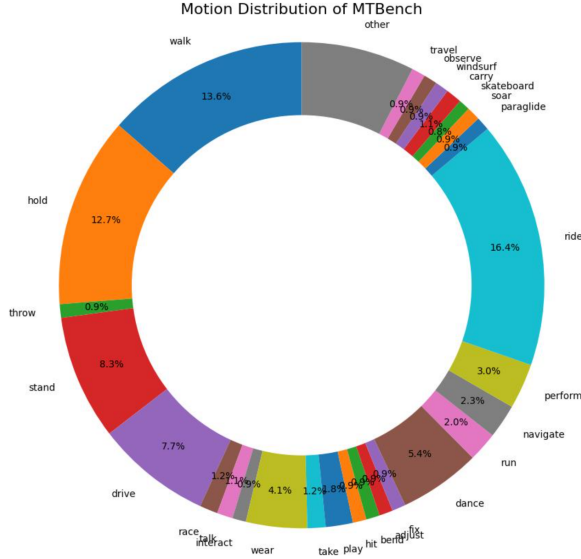


Figure 21. Motion Distribution of MTBench.

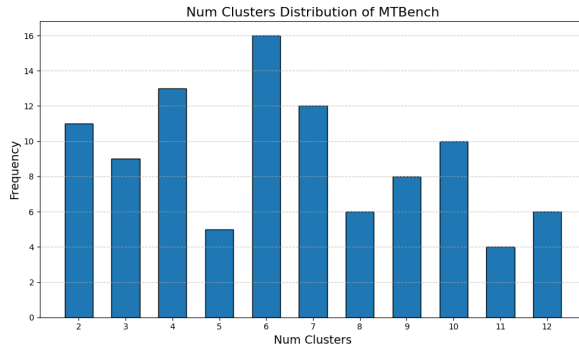


Figure 22. Num Clusters (Difficulty) Distribution of MTBench.

could serve as a potential decoupling method.

11. Additional Related Works

Controllable video generation. To better meet user demands, previous works [7, 39, 49, 51] have incorporated additional control signals into the video generation process, including control over the first frame [6], motion trajectories [61], object regions [53], and object identity [46, 52].

Specifically, trajectory-controlled methods guide subject movement through per-frame coordinates but lack fine-grained motion control. Region-controlled methods use bounding boxes to constrain subject positions in each frame, yet they still struggle to generate complex motions. Additionally, recent works [64] employ video masks to regulate motion. While masks effectively guide motion generation, they also restrict subject appearance, reducing text controllability.

In this work, we propose a tuning-based motion transfer

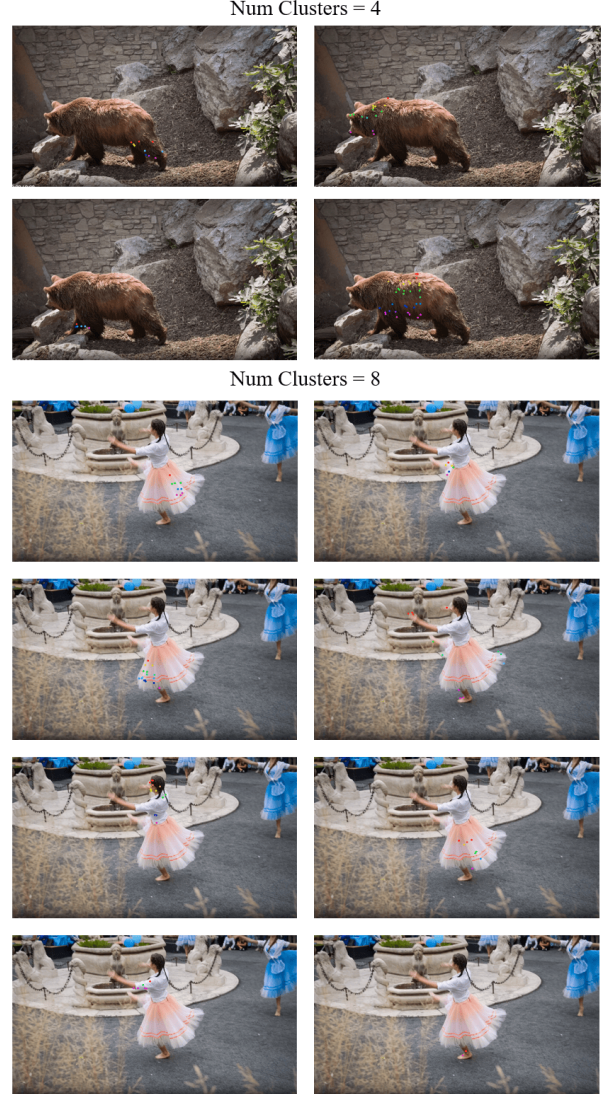


Figure 23. Visualization of Clusters.

method for DiT models, where the generated videos follow the motion of the source video while maintaining strong text controllability.

12. Limitations and Future Work

The success of DeT relies on two key assumptions.

First, the foreground and background DiT features must be separable in high-dimensional space. If this condition holds, smoothing along the temporal dimension can help the model better distinguish between foreground and background. However, if these features are not separable in high-dimensional space or remain indistinguishable within a given temporal window defined by the kernel size, then temporal smoothing alone will be ineffective. In such cases, the model may still memorize background appear-

ance, leading to overfitting.

Second, our assumption regarding the dense point tracking loss is that the key regions of foreground motion are already present in the first frame. This enables CoTracker to track foreground motion throughout the sequence. However, if critical motion-related parts are absent in the first frame—for example, a hidden hand—then the effectiveness of the dense point tracking loss may be reduced.

In the future, we will continue to enhance the model’s ability to decouple and learn motion. While the shared temporal kernel handles both tasks simultaneously, designing dedicated modules for decoupling and motion learning separately may further improve overall performance.